

# Local Maps Fusion for Real Time Multirobot Indoor Simultaneous Localization and Mapping\*

Diego Rodriguez-Losada, Fernando Matia and Agustin Jimenez

DISAM

Universidad Politecnica de Madrid

28006 Madrid, Spain

{drodri, matia & ajimenez}@etsii.upm.es

**Abstract**— This paper presents an implementation of the Local Maps Fusion concept for the Simultaneous Localization and Mapping (SLAM) problem within the Extended Kalman Filter (EKF) framework. Several problems never addressed before, arise while implementing the solution for indoor environments, and are successfully solved to obtain maps of quite large real indoor environments with more than one robot in real time.

**Keywords** - SLAM, EKF, multirobot, realtime, indoor.

## I. INTRODUCTION

The ability of a robot of building a map (see [1] for a survey on robotic mapping) of its environment while localizing itself in that map is an essential capability to reach true autonomy. Since the seminal paper [2], the EKF approach to the SLAM problem has been the most extended and the focus of many researchers.

Many authors ([3], [4], [5], [6], [7], [8] among them), try to improve the computational complexity of the EKF solution, well known to be  $O(n^2)$ , where ‘n’ is the number of map objects, obtaining great reductions while maintaining the optimality of the filter. The key idea is to maintain the optimal estimation in real time for a subset of features, and to accumulate the not applied correction, so it can be transferred to the whole map as a background process when desired. The approach of building a local map for storing that correction and using it as a compound observation for fusing it into the global map [3], [4], [5], is used in this paper.

Most of them use the point as the main kind of feature of the environment, mainly because handling a point in the EKF framework is simple, but also because using points is representative enough for the existing features (trees, corners). But this is not the case of an indoor environment where the most common feature is the segment (walls). An adequate representation for this kind of environment that inherits from the SPMMap [9] was developed in [10] and has been used in this implementation too (Section II).

While many of the above authors state that their algorithms are useful for handling multiple robots, there is a lack of experiments in real indoor environments that address simultaneously the representation of segments and the computational complexity, as well as handling multiple robots. Recently [11] implements a multirobot SLAM-EKF system for an indoor environment, but without real results in large environments neither handling real time constraints.

Several problems, first addressed in this paper, arise while implementing this Local Maps Fusion (LMF) approach, but it has been possible to overcome them (Section III), so real time experiments in actual quite large indoor environments are carried out (Section IV) with success. These experiments are done with multiple robots and a single centralized map.

## II. MULTIROBOT MAPPING: LOCAL MAPS FUSION (LMF)

### A. Representation

While a robot can be represented with a reference frame attached to it, the segments contain information for the EKF only in two dimensions: the angular and lateral displacement. Our solution for dealing with this uncertainty partiality, which inherits from the SPMMap [9], is described with detail in [10]. The main idea is that the state of every feature  $\bar{x}_F$  is decomposed in the estimation of its state  $\hat{x}_F$  and an error vector  $\bar{e}_F$  that accounts for the difference between this estimation and the actual state of the object. The state vector of every object contains a reference frame  $\vec{r}_F$  attached to it and some objects might require extra parameters for its representation (e.g. a segment is modeled by a reference frame in its midpoint and its length). A simplification (Fig.1) of this model will be used along this paper. Equation (1) shows the error vectors for a robot R and a segment S.

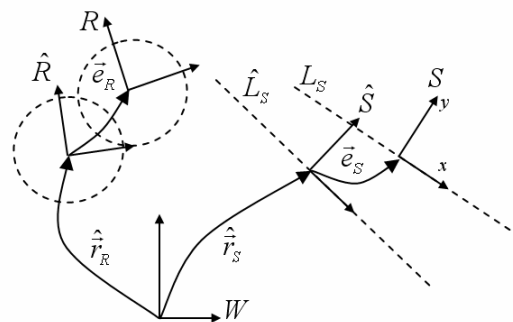


Figure 1. Objects representation with error vectors

This error vector has adequate dimension for representing the uncertainty of that object, and is the stochastic variable modeled as Gaussian and estimated by the EKF. The error vector estimation will be maintained with zero mean (1). This object representation is used both in the local and global maps.

\* This work is funded by Spanish Ministry of Science and Technology (URBANO: DPI2001-3652C0201) and EU 5th R&D Framework Program (WebFAIR: IST-2000-29456) and supervised by CACSA (Ciudad de las Artes y las Ciencias de Valencia)

$$\begin{aligned}
\bar{x}_R &= [\bar{r}_R] & \bar{e}_R &= [e_R^x \quad e_R^y \quad e_R^\theta]^T \\
\bar{x}_S &= [\bar{r}_S \quad L_S]^T & \bar{e}_S &= [e_S^y \quad e_S^\theta]^T \\
\bar{e}_{F_i} &\sim N(\hat{\bar{e}}_{F_i} = \bar{0}, P_{F_i} = Cov(\bar{e}_{F_i}, \bar{e}_{F_i}))
\end{aligned} \tag{1}$$

### B. Local Maps

In a particular time step, there are ‘n’ robots simultaneously building the map. Each one builds its own local map relative to its own local reference frame. The local map of robot number ‘r’ contains only one robot, and ‘k<sub>r</sub>’ segments. The number of objects ‘k<sub>r</sub>’ of a local map increases as new segments are seen.

$$\begin{aligned}
\hat{x}_{Mr} &\triangleq \left[ \left( \hat{x}_R^{Lr} \right)^T \quad \left( \hat{x}_{S1}^{Lr} \right)^T \quad \dots \quad \left( \hat{x}_{S_{k_r}}^{Lr} \right)^T \right]^T \\
\hat{e}_{Mr} &= \bar{0} ; P_{Mr} \triangleq \left[ Cov(\bar{e}_i, \bar{e}_j) \Big|_{i,j=0\dots k_r} \right]
\end{aligned} \tag{2}$$

Each local map is computed following the algorithm described in [10] which include the handling of segments within EKF, the use of geometric shape constraints for indoor environments, an incremental joint compatibility test, the geometric update of the features, multiple pairings per observation (not nearest neighbor approach), and fusing separate features that match a single actual object.

As established in [4], [5] the estimation of each local map is decorrelated from the rest of the global map, and can be maintained with a computational cost of O(k<sup>2</sup>), being ‘k’ small enough to maintain real time performance.

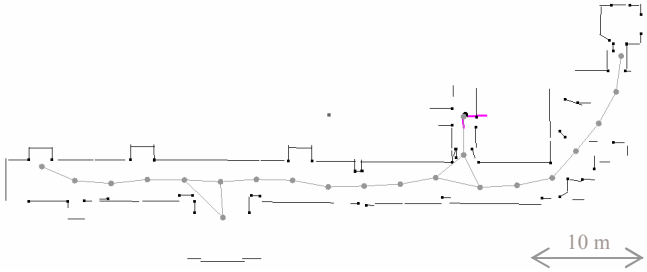


Figure 2. University corridor map built on line by remote operation

With our implementation, the maximum number of features that can be handled in real time by a robot is 170, but smaller maps can be perfectly built in real time. In fact, it has recently been done the ‘‘Explore and return’’ experiment [12], but in a larger environment, mapping 106 objects. The robot was operated remotely in an indoor populated environment with the only help of the map being built and the sensor readings (i.e. without direct sight to the robot), while performing real time map building and computing the graph of the environment. This graph shown in Fig. 2 was used to return home, but also to plan and execute movements in already known areas as an aid for the robot remote operation. The distance traveled was 134 meters in 22 minutes. Our approach described in [10] was used for an efficient handling of the segment edges. The local maps size (10-20m) used in the LMF approach is typically much smaller than this map and the processing time as little as 10 ms per update step, so they can be handled in real time with no problem at all.

### C. Fusing Local Maps

The global map is defined by ‘n’ references frames of the local maps and by ‘m’ segments previously added to the map.

$$\begin{aligned}
\hat{x} &\triangleq \left[ \left( \hat{x}_{L1} \right)^T \quad \dots \quad \left( \hat{x}_{Ln} \right)^T \quad \left( \hat{x}_{S1} \right)^T \quad \dots \quad \left( \hat{x}_{Sm} \right)^T \right]^T \\
\hat{e} &= \bar{0} ; P \triangleq \left[ Cov(\bar{e}_i, \bar{e}_j) \Big|_{i,j=1\dots n+m} \right]
\end{aligned} \tag{3}$$

When a robot decides to fuse the information of its local map with the global map, the information of the local map ‘r’ is transferred to the global map. The local map ‘r’ is initialized, the features are deleted and the robot restarts its operation at position 0 with uncertainty (covariance matrix) 0. The local map ‘r’ keeps being built in real time.

A background task is launched for fusing the local map into the global one. First of all, the global state estimation is augmented with the local one, so due to the decorrelation of the local map, the new augmented estimation and error covariance are:

$$\hat{x}^- \triangleq \begin{bmatrix} \hat{x} \\ \hat{x}_{Mr} \end{bmatrix}; \hat{e}^- \triangleq \begin{bmatrix} \hat{e} \\ \hat{e}_{Mr} \end{bmatrix}; P^- \triangleq \begin{bmatrix} P & 0 \\ 0 & P_{Mr} \end{bmatrix} \tag{4}$$

Then, several implicit measurement equations are done. As all the variables are included in the state, these implicit measurement equations are equivalent to the constraints [6] defined in [4], [5]. The implicit measurement (Fig.3) that relates the global map segment  $S_i$  with the local map segment  $S_j^{Lr}$  is represented conceptually by (5).

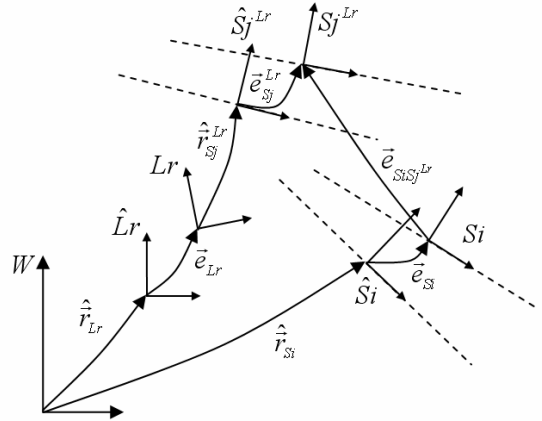


Figure 3. Implicit measurement equation for the local map fusion.

$$\vec{h}_{SiSj^{Lr}} = \vec{e}_{SiSj^{Lr}} = \left( \ominus \bar{x}_{Si}^{Lr} \oplus \bar{x}_{Lr} \oplus \bar{x}_{Sj} \right) = \bar{0} \tag{5}$$

This equation has to be properly formulated with error vectors (6) within the proposed framework.

$$\vec{h}_{SiSj^{Lr}} = B \left( \ominus \begin{bmatrix} 0 \\ \bar{e}_{Si} \end{bmatrix} \ominus \hat{r}_{Si} \oplus \hat{r}_{Lr} \oplus \bar{e}_{Lr} \oplus \hat{r}_{Sj}^{Lr} \oplus \begin{bmatrix} 0 \\ \bar{e}_{Sj}^{Lr} \end{bmatrix} \right) = \bar{0} \tag{6}$$

Matrix B is a selection matrix formed by the last 2 rows of the 3x3 identity matrix. The theoretical value of the measurement vector (6) should be zero, but the actual value

that is obtained when substituting the actual estimation of the error vectors (7) is not equal zero and conceptually equivalent to the innovation. The jacobians of (6) are computed (7) to obtain the innovation covariance, and are stored for the joint compatibility test and EKF update steps.

$$\hat{h}_{SiSj^{Lr}} = \bar{h}_{SiSj^{Lr}} \Big|_{(\bar{e}_{Lr} \rightarrow \hat{e}_{Lr} = \bar{0}; \bar{e}_{Sj} \rightarrow \hat{e}_{Sj} = \bar{0}; \bar{e}_{Sj}^{Lr} \rightarrow \hat{e}_{Sj}^{Lr} = \bar{0})} \neq \bar{0}$$

$$H_{SiSj^{Lr}} = \frac{\partial \bar{h}_{SiSj^{Lr}}}{\partial \bar{e}^-} = \begin{bmatrix} 0 & \frac{\partial \bar{h}_{SiSj^{Lr}}}{\partial \bar{e}_{Lr}^-} & 0 & \frac{\partial \bar{h}_{SiSj^{Lr}}}{\partial \bar{e}_{Sj}^-} & 0 & \frac{\partial \bar{h}_{SiSj^{Lr}}}{\partial \bar{e}_{Sj}^{Lr}^-} & 0 \end{bmatrix} \quad (7)$$

*with*  $(\bar{e}_{Lr}^- \rightarrow \hat{e}_{Lr}^- = \bar{0}; \bar{e}_{Sj}^- \rightarrow \hat{e}_{Sj}^- = \bar{0}; \bar{e}_{Sj}^{Lr} \rightarrow \hat{e}_{Sj}^{Lr} = \bar{0})$

The implicit measurement equations have to pass a single Mahalanobis distance test (8) to accept the pairing. Contrary to the nearest neighbor approach, multiple pairings from a single observation must be allowed [10] as long as they satisfy the test.

$$C = \text{Cov}(\hat{h}_{SiSj^{Lr}}) = H_{SiSj^{Lr}} P^- H_{SiSj^{Lr}}^T \quad (8)$$

$$\text{if} \left( \hat{h}_{SiSj^{Lr}}^T C^{-1} \hat{h}_{SiSj^{Lr}} < \chi^2_{\text{dim}(\hat{h}_{SiSj^{Lr}}), \alpha} \right) \Rightarrow \text{Accepted}$$

Then, an incremental joint compatibility test [13] is applied to the set of equations that have passed the single Mahalanobis test. The equations that are not compatible with the rest are discarded and the EKF correction is applied in a single with all the compatible equations. The joint innovation vector is obtained by concatenating the single innovations, as well as the joint Jacobian matrices to compute the innovation covariance matrix S, the Kalman gain W and to apply the EKF update step. This is the most expensive operation of the algorithm with a computational cost of  $O(m^2)$ , (n discarded:  $n \ll m$ ).

$$\hat{h} = \begin{bmatrix} \vdots \\ \left( \hat{h}_{SiSj^{Lr}} \right)_l \\ \vdots \end{bmatrix}; \quad H = \begin{bmatrix} \vdots \\ \left( H_{SiSj^{Lr}} \right)_l \\ \vdots \end{bmatrix}$$

$$S = HP^-H^T; \quad W = P^-H^T S^{-1}$$

$$\hat{e}^+ = -W\hat{h}; \quad (9)$$

$$\hat{x}^+ = \hat{x}^- \odot \hat{e}^+ \Rightarrow \hat{e} \triangleq \bar{0}$$

$$P^+ = P^- - WHP^-$$

After the correction step, the geometric update of the map is done with the geometric information of the paired observations that is not handled by the EKF. This is accomplished projecting the local map segments onto their (already updated by the EKF) paired map segments, computing new lengths and midpoints for them. The local map features that are used in the EKF update step are then deleted from the state, and the global map features that matched the same local map feature are fused together in a single one. The local map reference frame is updated to the new robot 'r' position and covariance, and the robot is deleted from the global map. The background task ends and the global map is ready to perform another local map fusion.

### III. IMPLEMENTING LMF

The formulation presented above, is used in the experiments in [3], [4] and [5] with success. Nevertheless, those experiments were carried out in not enough large environments, and are not a sufficient proof of the behavior of the algorithm. A naïve implementation of the above formulation has been tested. When trying to build the maps with this formulation, several problems (first addressed in this paper) arise, that makes the algorithm to produce unexpected bad results. These problems are much bigger when the robots revisit already mapped places, so most of the features of the local maps match the features of the global map. In fact, the mapping for the first time, while the robots continuously explore new places and only few features of each local map are paired with the global map, is perfectly done. The problems are clearly visible when the robots revisit old places and most of their local maps match the global one.

#### A. Avoiding Inconsistency

The first problem is that the pairings that are supposed to be established in the data association step are not paired, the global map is not corrected, new features are added, and the global map diverges. The main reason for this behavior is that the single Mahalanobis distance test is not passed, due to the unexpected low covariance matrices of both the local and global map.

The properties of consistency and convergence are proved in [12] and extended to multirobot systems in [11] with the assumption of linear equations, but as described in [14] and accepted in [12], the SLAM problem based on a EKF for estimation is inconsistent and divergent due to the structural problem of the linearization in presence of large angular errors. The experiments done in [14] are extended to show that this effect increases with the angular covariance of the robot. The simulation starts with a robot at zero position and orientation that observes a new object (with 3D information, i.e. x-y position and orientation) and adds it to the map. The initial covariance is 0 for the robot position and varies from 0.005 to 0.03 for the robot orientation (measured in radians). It can be seen in figure 2 that a larger initial covariance implies a larger inconsistency and a more likely bigger spurious correction. The fact is that these values of covariance can be reached within a few meters of robot displacement if not enough features are available to maintain the robot orientation covariance small enough. The spurious angle corrections produce a large position error after several meters of robot movement.

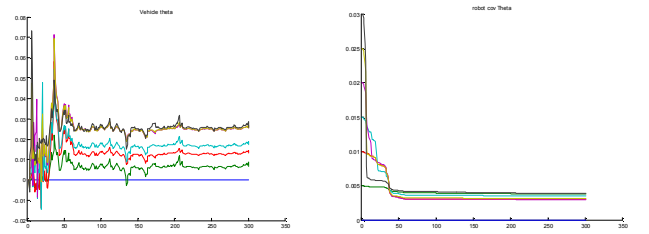


Figure 4. Angular error (left) and covariance (right) vs timestep.

The easiest solution for this problem is to minimize the angular uncertainty of the robot without letting it to grow

without bound. Some authors [14] propose the use of a compass to get an absolute reference of orientation. When mapping indoor structured environments it is very convenient to use a priori map knowledge shape constraints: parallelism, perpendicular and/or colinearity. In [12] virtual observations between objects of the map are done with large uncertainty, while [10] applies perfectly known constraints between the objects added in the last step and the rest of the objects. The latter is the approach used in this paper.

Using constraints, the local map estimation is consistent and convergent, and the LMF Mahalanobis single-pairing test is satisfied, but a new problem appears as described below.

### B. Inverting the innovation covariance matrix

The innovation vector is composed by all the innovation vectors of the pairings that have passed the single compatibility test, and the jacobian matrix H accumulates the jacobians of the measurement equation of each pairing (9). With this matrices, the innovation covariance S is computed. The innovation covariance must be inverted to apply the EKF update step. If the inversion is carried out without any check and the update is done, the result is a large divergence of the map and a clear loss of positive semidefiniteness of the covariance matrix P. The problem arises because the matrix S is highly ill-conditioned. As described in [6] the use of constraints inside the EKF framework produce the “flattening” of the ellipsoid of the covariance matrix of the state onto the constraint surface, i.e. the determinant of the covariance matrix P when using constraints is equal 0.

$$\det(\mathbf{P}_{Mr}) = 0 \Rightarrow \det(\mathbf{P}) = 0 \quad (10)$$

Conceptually, this means that at least one relative transformation between two of the objects of the local map is perfectly known. If this perfect known relative transformation is transferred to the global map the resulting covariance matrix also inherits this property. This happens when the two objects that appear in that relative transformation are considered as new objects because are not matched against any object in the global map. This always occurs when the robot is exploring new areas, so it is an unavoidable behavior (10). It is important to note that these conditions will also occur as the global map converges [6], and if the local map becomes highly correlated due to a long stay of the robot in the same area.

When the data association of the local map fusion is done it is very likely that several pairings will be established, especially when revisiting already mapped places. If two different pairings match a perfectly known relative transformation both in the local and in the global map, it is guaranteed that the obtained innovation covariance matrix S will be absolutely ill- conditioned.

It could be argued that a “single pairing at a time” approach will overcome the problem. This could be true, but as described in [4] one of the main advantages of the Local Maps Fusion approach is that the data association step can be done more robustly. This robustness is achieved with a Joint Compatibility Mahalanobis distance test. No matter if the covariance matrix is inverted incrementally [13] or not, it has to be inverted to do such a test.

So, without applying constraints, the result is inconsistent and divergent, and if applying constraints or in the limit when many observations are done, the covariance matrix is ill-conditioned. Let’s say that there is an “information overflow” in this matrix. To solve this problem, a careful matrix inversion is done.

The covariance matrix is inverted with full pivot Gauss Jordan elimination [15]. The errors due to the condition of the matrix can be easily detected when the chosen pivot becomes small. At this point the matrix inversion is stopped. The rows and columns containing the pivots that have already been used in the matrix inversion are the independent information, while the unused ones represent the information that is redundant in the covariance matrix. The latter ones are used to delete the respective innovation vector components and jacobian H respective rows. The dimension of all matrices now agree for their use in the Joint Compatibility test and in the EKF update step, and the covariance matrix inversion is guaranteed to be free of numerical errors.

### C. Using Local Reference Frames

There is another problem that does not produce a catastrophic failure of the algorithm but a deformation of the shape of local areas of the map. The source of this error is the low correlation between perpendicular segments and the existence of large corrections when closing loops or revisiting already mapped places. Fig. 5 shows how the university map is locally deformed by a large correction.



Figure 5. Map details before (left) and after (right) a large correction

To solve this problem it is very convenient to maintain submaps, each one with its own local reference frame. With this approach, the ‘m’ global map segments are grouped into ‘p’ submaps, each one containing the reference frame F of all the ‘k<sub>i</sub>’ segments that are in that submap. The full covariance matrix P is still maintained, storing the correlations between all entities of the map and maintaining also the linear optimality of the filter.

$$\hat{\mathbf{x}} \triangleq \begin{bmatrix} \hat{\mathbf{x}}_{L1}^T & \cdots & \hat{\mathbf{x}}_{Ln}^T & \hat{\mathbf{x}}_{Fi}^T & (\hat{\mathbf{x}}_{S1}^{Fi})^T & \cdots & (\hat{\mathbf{x}}_{Sk_i}^{Fi})^T \end{bmatrix}^T \quad (11)$$

$$\forall i = 1, \dots, p; \quad \sum_{i=1}^p k_i = m$$

The algorithm for building the robot local maps remains unmodified, but the implicit measurement equations for the map fusion (12) has to take into account the new local reference frame ‘F<sub>n</sub>’ of the map segment ‘S<sub>i</sub>’. See [4] for a more detailed description of the constraints when using local frames.

$$\bar{\mathbf{h}}_{SiSj^r} = \mathbf{B} \left( \ominus \begin{bmatrix} \mathbf{0} \\ \bar{\mathbf{e}}_{Si}^{Fn} \end{bmatrix} \ominus \hat{\mathbf{r}}_{Si}^{Fn} \ominus \bar{\mathbf{e}}_{Fn} \ominus \hat{\mathbf{r}}_{Fn} \oplus \hat{\mathbf{r}}_{Lr} \oplus \bar{\mathbf{e}}_{Lr} \oplus \hat{\mathbf{r}}_{Sj}^{Lr} \oplus \begin{bmatrix} \mathbf{0} \\ \bar{\mathbf{e}}_{Sj}^{Lr} \end{bmatrix} \right) \quad (12)$$

A side advantage of using local reference frames for the objects is that these references frames represent the graph of the environment. By simple considerations when performing the data association step of the local map fusion algorithm, it is very easy to connect the corresponding reference frames so an approximate graph of the environment is obtained. This graph can be very useful for exploration or navigation purposes.

#### IV. EXPERIMENTS

Only one robot was available for the experiments, so several different trajectories were manually operated and the data was saved with the corresponding timestamps. This data is afterwards fed into the LMF mapping application in real time, as if the robots were actually operating simultaneously. To proof the flexibility of the implementation, the robots can join the mapping “on the fly”, i.e. robots can be dynamically added to the LMF. When a robot performs a relative observation of another robot, the new robot can join and start to collaborate in the mapping. This robot-robot observation is the only simulation done in the whole approach. Two different robots are used for the exploration, a Pioneer robot for the first experiment and a B21r for the second one, both of them equipped with a Sick laser scanner. This laser refreshes at 5Hz, so the maximum elapsed time between consecutive scans must be less than 200 ms to guarantee real time performance.

A split and merge algorithm followed by a least squares fit is used for extracting the segments from the laser raw data. The error of each range measure point is about +5 cm. The odometry error is considered to be proportional to the incremental movement and is about 6% for the B21 and 8% for the Pioneer robot.

The software has been done in C++ with extensive use of the STL. The standard optimizations described in [7], using the sparsity of the matrices, are extended to the local maps fusion to obtain a computational cost of  $O(m^2)$  of the fusion step. The computation is carried out on a single P4 2,4GHz PC under WinXP, both the global map fusing and building the local map of each robot. Of course the OS does not guarantee real time strictly but the obtained results are satisfactory enough to show the effectiveness of the approach.

Two experiments in two quite large indoor environments are carried out. In both experiments, each robot explores new areas, but also revisits the areas mapped by the other robots. The local maps size is chosen to be 10 meters, when the local map of a robot exceed this dimension is fused with the global

map. This fusing is done as a background process (low priority thread), so if the fusing task is active, the robot keeps building the local map and delays the fusing until the fusing task is idle.

The first experiment uses 2 Pioneer robots to map Belgoioso castle in Italy. Both of them start at the same time to map the environment. The distances traveled are 158 meters in 12 minutes and 133 meters in 9 minutes respectively. The 239 objects map (including robots and local reference frames) and the environment graph are showed in fig 6. Two large loops of 100 meters each are correctly closed in this experiment.

In the second experiment, the populated university ground floor is mapped with 3 B21r robots. The first one starts moving and soon observes the second robot. Each one takes an opposite direction. After a while, the second robot sees the third one that start to collaborate, mapping the leftmost corridor of the map. Robot 1 travels 319m in 20min, robot 2 travels 268m in 16min and robot 3 travels 380m in 19min. Figure 7 shows the map build as well as the generated graph environment. The total number of objects of the map is 270, including the robots and the local reference frames. As the actual trajectory of the robots makes the figure confusing, the schematic path of the robots is shown. A large loop of 100m is correctly closed in this experiment. As the segments position is relative to the local reference frame, figures 6 and 7 show instead their absolute projected position.

The elapsed time between two consecutive updates, for the odometry and the laser is shown in Fig. 8. It can be seen that the 200 ms bound is not infringed, so this experiment is successfully accomplished within the real time constraints. Experiment one also accomplishes the real time performance but the time graph is not displayed for space reasons. The covariance matrix is supervised along the process to check that there is no lost of positive semidefiniteness.

A known limitation of this approach is the computational cost increase with the size of the submaps due to the joint compatibility test. The incremental joint compatibility uses an heuristic that improves the computational complexity, but that can still be too large if many pairings satisfy the single test.

Larger environments can also be mapped in real time with this approach. The size of the map that can be handled in real time depends on the number of robots and their speed, the local maps size and the density of features.

More information about these experiments at: <http://www.disam.upm.es/~drodri>

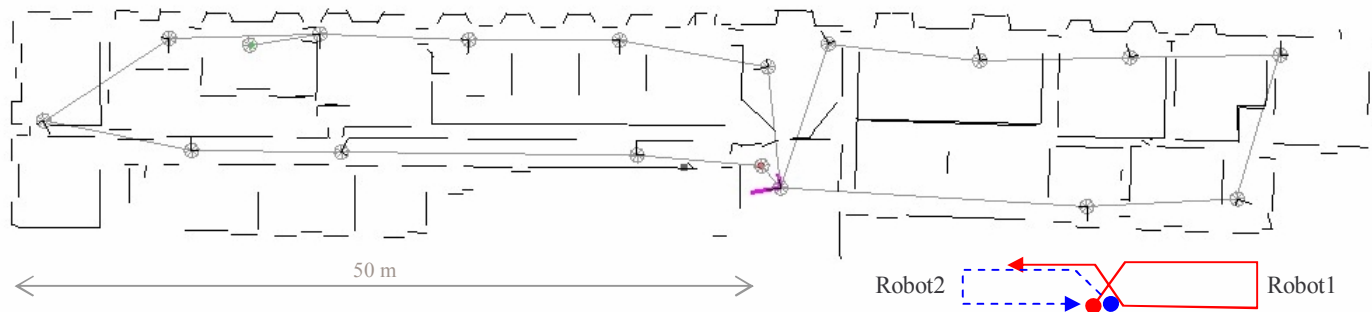


Figure 6. Belgoioso Castle map built in real time with 2 Pioneer robots

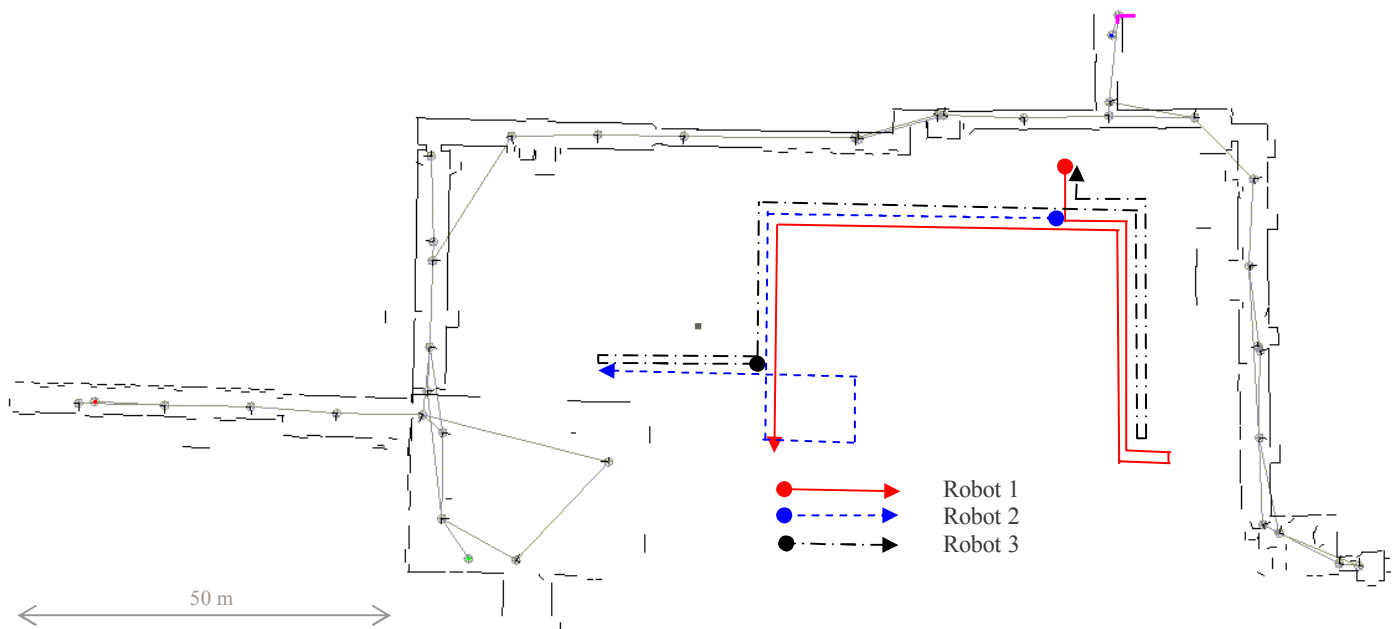


Figure 7. University Map built in real time with 3 B21r robots; robot trajectories

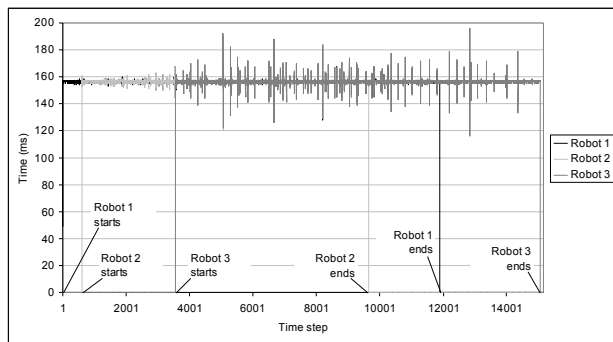


Figure 8. Elapsed time between consecutive updates

## V. CONCLUSIONS AND FUTURE WORK.

This paper has presented a solution for the real time multirobot SLAM problem based on an EKF and the local maps fusion concept for handling large environments. Several problems never addressed before have been found and successfully solved. Real time performance, the correctness of the solutions and the multirobot implementation are tested with real experiments in two different indoor environments using different robots with excellent results. Future work includes the implementation of autonomous exploration strategies for indoor environments as well as on line experiments with several robots, as well as an extension to 3D, handling dynamics (doors) and adding new kinds of objects. A new high level reasoning module based on geometry will be added.

## REFERENCES

[1] S. Thrun. "Robotic mapping: A survey" In G. Lakemeyer and B. Nebel, editors, *Exploring Artificial Intelligence in the New Millenium*. Morgan Kaufmann, 2002

[2] R. Smith, M. Self and P. Cheeseman "Estimating uncertain spatial relationships in robotics" in *Uncertainty in Artificial Intelligence 2*, J.F. Lemmer and L. N. Kanal, Eds. New York: Elsevier, 1988

[3] J.D. Tardos, J. Neira, P. Newman, J.J. Leonard "Robust Mapping and Localization in Indoor Environment using Sonar Data" MIT Marine Robotics Laboratory Technical Memorandum 0-14. Unpublished.

[4] Williams, Stefan. PhD dissertation: "Efficient Solutions to Autonomous Mapping and Navigation Problems" Australian Center for Field Robotics, University of Sidney 2001.

[5] S. Williams, G. Dissanayake, and H.F. Durrant-Whyte. "An efficient approach to the Simultaneous Localization and Mapping Problem" . ICRA02 Washington DC, 15(5), 2001, pages 406-411

[6] Newman, Paul. PhD dissertation: "On the Structure and Solution of the Simultaneous Localisation and Map Building Problem". Australian Center for Field Robotics, University of Sidney 1999

[7] Guivant J, and E. Nebot, "Optimization of the Simultaneous Localization and Map-Building Algorithm for Real-Time Implementation" IEEE transactions on robotics and automation, vol. 17, no. 3, june 2001 p242-257

[8] Knight, J.; Davison, A.; Reid, I.; "Towards constant time SLAM using postponement" IEEE/RSJ Int. Conf. on Intelligent Robots and Systems, 2001. Hawaii, USA Vol: 1, Page(s): 405 -413

[9] J.A. Castellanos, J.M.M. Montiel, J. Neira and J.D. Tardós, "The SPMAP: A Probabilistic Framework for Simultaneous Localization and Map Building.", IEEE Transactions on Robotics and Automation, Vol. 15, No. 5, pp. 948 - 953, October 1999

[10] Rodriguez-Losada, D.; Matia, F. "Integrating segments and edges in feature-based SLAM" . IEEE Int. Conf. on Advanced Robotics 2003. Coimbra, Portugal.

[11] Fenwick, J.W.; Newman, P.M.; Leonard, J.J. Cooperative concurrent mapping and localization ; IEEE Int. Conf. on Robotics and Automation, 2002. Washington, DC Vol: 2 , 11-15 Page(s): 1810 -1817

[12] P. Newman J. Leonard, J. D. Tardos, J. Neira "Explore and Return: Experimental Validation of Real-Time Concurrent Mapping and Localization" IEEE Int. Conf. on Robotics and Automation, 2002. Washington, DC, p 1802-1809

[13] J. Neira and J.D. Tardos, "Data association in stochastic mapping using the joint compatibility test" IEEE Trans. on Robotics and Automation, vol. 17, no. 6, pp. 890-897, 2001.

[14] Julier, S.J.; Uhlmann, J.K "A counter example to the theory of simultaneous localization and map building.;" IEEE Int. Conf. on Robotics and Automation, 2001, Seoul, Korea, Vol4 ,Page(s): 4238 -4243

[15] W.H. Press, S.A. Teukolsky, W.T. Vetterling & B.P. Flannery, "Numerical Recipes in C" (2nd edition, 1992), Cambridge University Press, ISBN 0-52143108 -5